Light ALPs at Future Lepton Colliders

Shou-Shan Bao (鲍守山), Shandong University, ssbao@sdu.edu.cn

JHEP10(2025)122,
Collaborator: Yang Ma, Yongcheng Wu, Keping Xie and Hong Zhang

目录

CONTENTS

01 Introduction to ALPs

02 Current constraints

03 Long-lived ALP on Lepton Colliders

3.1 Mono-Photon Channel

3.2 Mono-Z Channel

3.3 Vector Boson Scattering

04 Conclusion

What Are Axion-Like Particles?

- The axion was first introduced by Peccei and Quinn to solve the strong CP problem.
- Axion-like particles (ALPs) are motivated by several theoretical considerations. They are pseudo-Nambu-Goldstone bosons arising from the spontaneous breaking of global U(1) symmetries. They are singlets of the SM gauge group and can couple to the gauge bosons.

- The mass range of ALPs is extremely broad, spanning from 10^-22 eV to the TeV scale. The long-lived ALPs can be the candidate of Dark Matter.

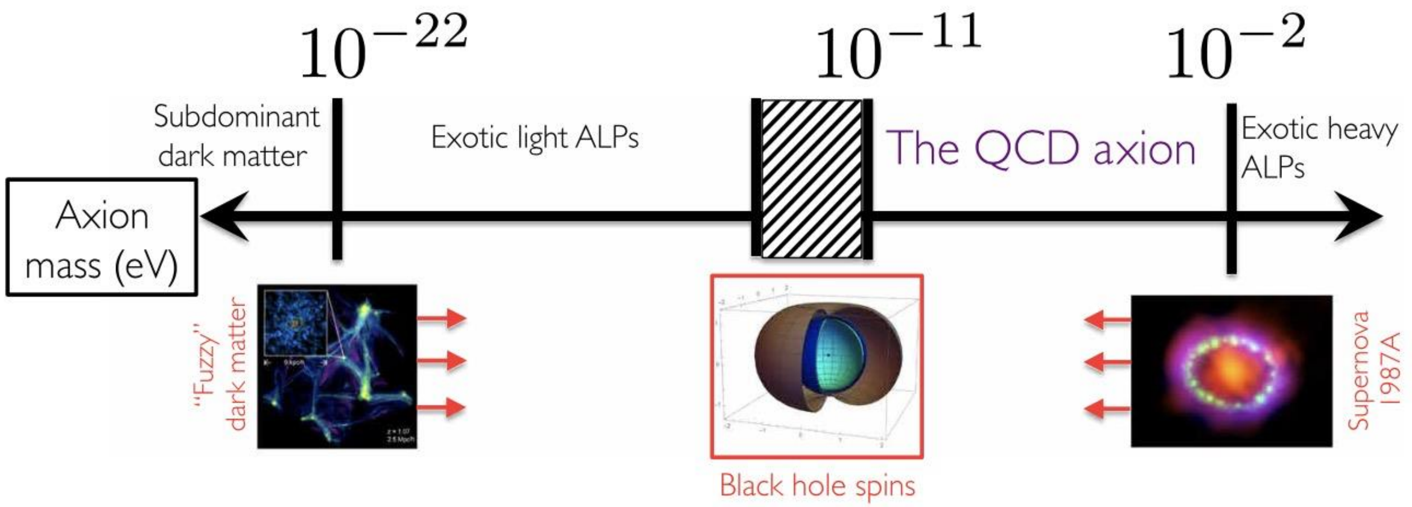

Effective Lagrangian for ALPs

Gauge invariant EFT

The SM gauge invariant effective Lagrangian describing the coupling of ALPs with gauge bosons is given as

$$\mathcal{L}_{\rm eff} \supset -C_G \frac{a}{f_a} G^b_{\mu\nu}\tilde{G}^{b;\mu\nu} - C_B \frac{a}{f_a} B_{\mu\nu}\tilde{B}^{\mu\nu} - C_W \frac{a}{f_a} \sum_{i=1}^{3} W^i_{\mu\nu}\tilde{W}^{i;\mu\nu};$$

a-gg coupling

The ALP-gluon coupling can be constrained through Mono-jet process [ATLAS, PRD 103, 112006 (2021)] and Mono-hadron production [**BSS**, WHGao, HZhang & JZhou, PRD110 (2024) 5, 055008]on LHC.

a-EW coupling

After electroweak symmetry breaking, the C_B and C_W translate into four physical couplings: gaγγ, gaγZ, gaZZ, and gaWW.

$$\mathcal{L}_{\rm eff} \supset -\frac{g_{agg}}{4} a G^b_{\mu\nu}\widetilde{G}^{b;\mu\nu} - \frac{g_{a\gamma\gamma}}{4} a F_{\mu\nu}\widetilde{F}^{\mu\nu} - \frac{g_{a\gamma Z}}{4} a F_{\mu\nu}\widetilde{Z}^{\mu\nu} - \frac{g_{aZZ}}{4} a Z_{\mu\nu}\widetilde{Z}^{\mu\nu} - \sum_{i=\pm} \frac{g_{aWW}}{2} a W^i_{\mu\nu}\widetilde{W}^{i;\mu\nu},$$

$$g_{a\gamma\gamma} = \frac{4}{f_a}(s_W^2 C_W + c_W^2 C_B), \quad g_{a\gamma Z} = \frac{8}{f_a} s_W c_W (C_W - C_B),$$
$$g_{aZZ} = \frac{4}{f_a}(c_W^2 C_W + s_W^2 C_B), \quad g_{aWW} = \frac{4}{f_a} C_W,$$

Lepton colliders offer clean environments to probe ALP interactions with electroweak bosons.

Current constraints on Long-lived ALPs

01 In this study, we focus on light ALP and assume Br(a → γγ) = 1 for long-lived ALPs.

$$\Gamma_a = \frac{g_{a\gamma\gamma}^2 m_a^3}{64\pi}. \qquad L_D = c\beta_a\gamma_a\tau_a = \frac{cp_a}{m_a\Gamma_a},$$

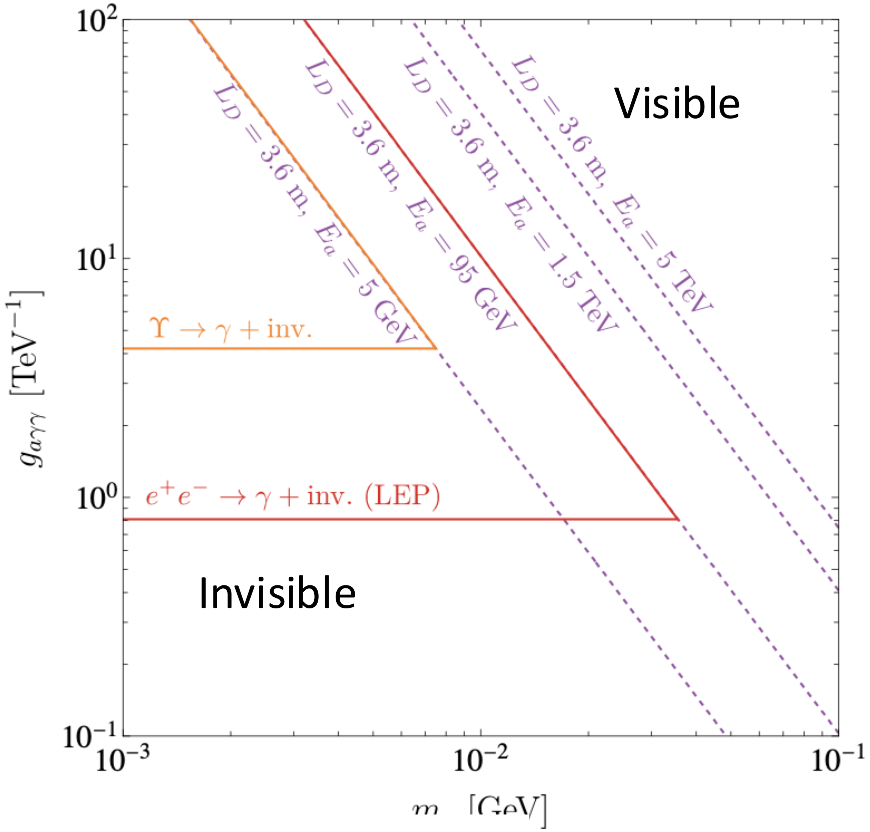

02 Experimental Signatures

- Hadron decay: $\text{Br}(\Upsilon \to \gamma + a) = \frac{g_{a\gamma\gamma}^2 m_b^2}{8\pi\alpha}\text{Br}(\Upsilon \to e^+e^-)$,

  E. Masso and R. Toldra, Phys. Rev. D 52 (1995) 1755

- Mono-photon: $\sigma_{\ell^+\ell^-\to\gamma a} = \frac{\alpha}{768}\left[32 g_{a\gamma\gamma}^2 + \frac{8 g_{a\gamma\gamma} g_{a\gamma Z}(c_W^2 - 3s_W^2)s}{s_W c_W (s - M_Z^2)} + \frac{g_{a\gamma Z}^2(6s_W^4 + 2c_W^4 - 1)s^2}{s_W^2 c_W^2 (s - M_Z^2)^2}\right]$,

  OPAL collaboration, Eur. Phys. J. C 18 (2000) 253

- Z invisible decay: $\Gamma(Z \to \gamma + a) = \frac{g_{a\gamma Z}^2}{384\pi} M_Z^3$.

$$g_{a\gamma\gamma} = \frac{4}{f_a}(s_W^2 C_W + c_W^2 C_B), \qquad g_{a\gamma Z} = \frac{8}{f_a} s_W c_W (C_W - C_B),$$

$$g_{aZZ} = \frac{4}{f_a}(c_W^2 C_W + s_W^2 C_B), \quad g_{aWW} = \frac{4}{f_a} C_W,$$

Current constraints on Long-lived ALPs

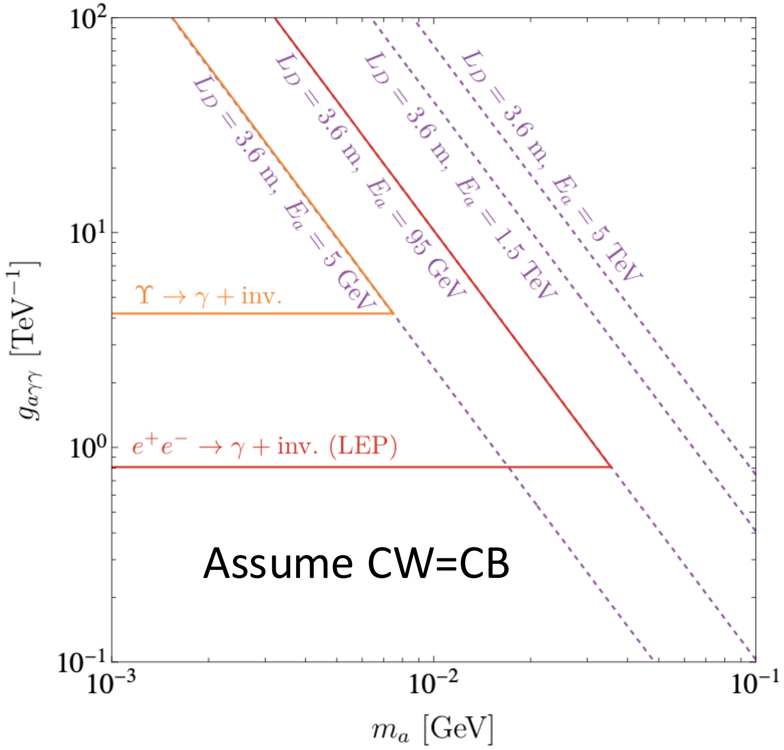

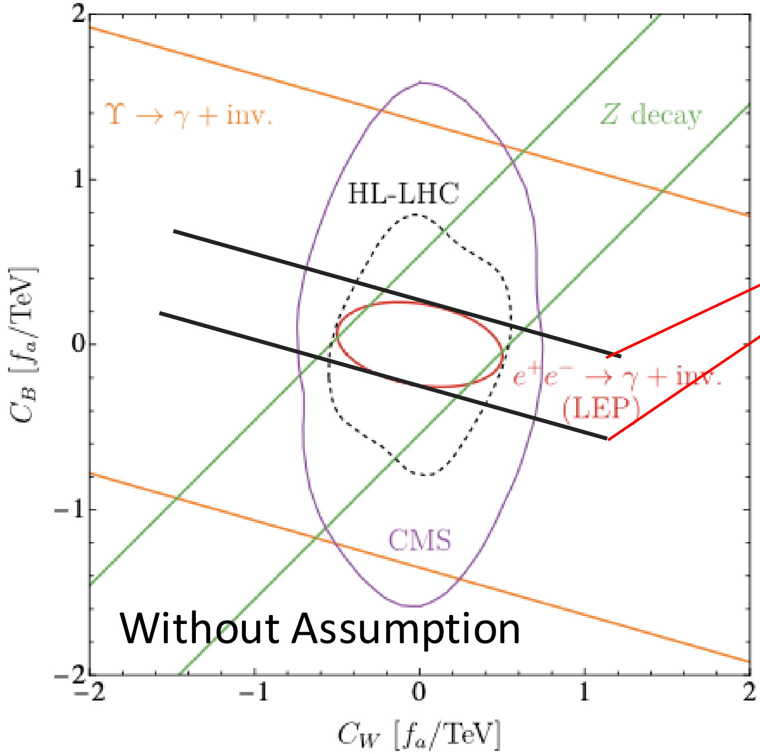

The constraint on the $g_{a\gamma\gamma}$

The constraints on the other physical couplings can be obtained in the same way.

$$g_{a\gamma\gamma} = \frac{4}{f_a}(s_W^2 C_W + c_W^2 C_B), \qquad g_{a\gamma Z} = \frac{8}{f_a} s_W c_W (C_W - C_B),$$

$$g_{aZZ} = \frac{4}{f_a}(c_W^2 C_W + s_W^2 C_B), \quad g_{aWW} = \frac{4}{f_a} C_W,$$

Mono-Photon Production

Production Process

ALPs can be produced in association with a photon. The process e+e− → γ + a leads to a mono-photon signature if the ALP is long-lived and escapes detection.

Background

The dominated background is from the e+e → γ + Z with Z decays to a pair of neutrinos.

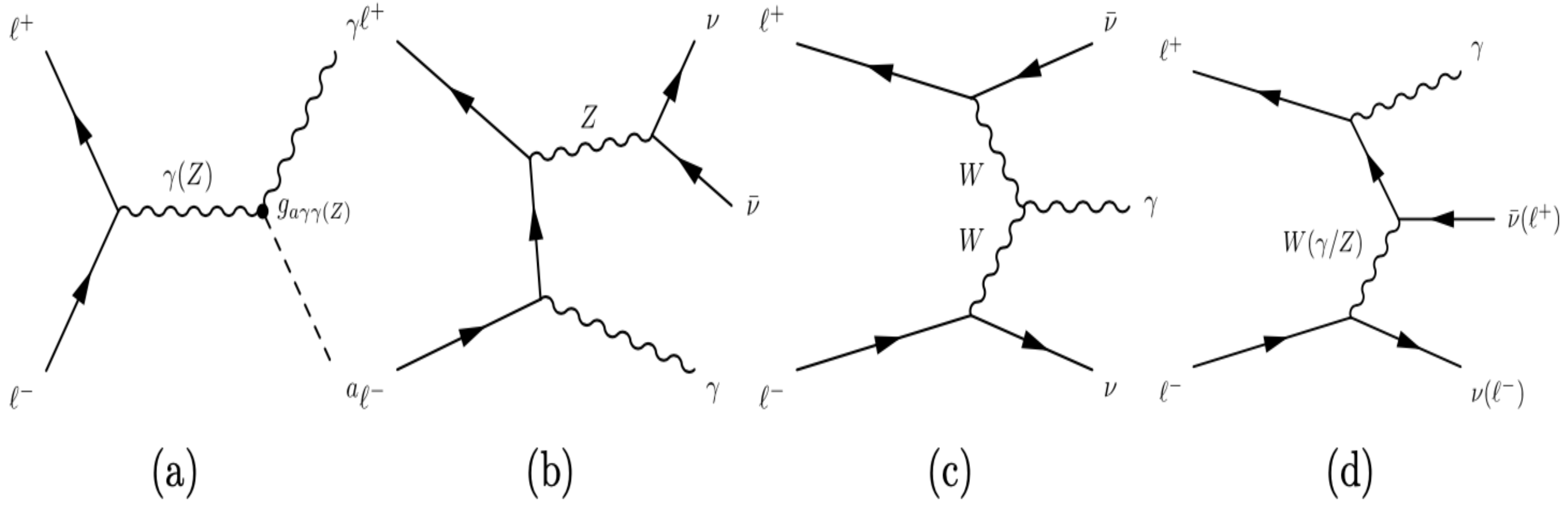

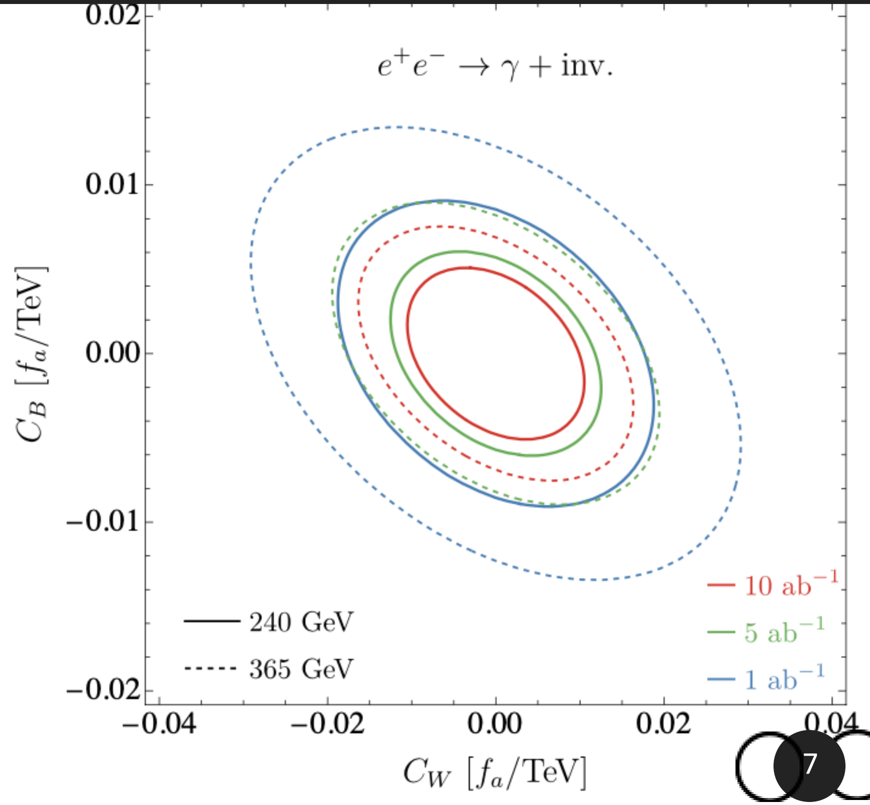

Mono-Photon Production

- The cut efficiency become lower for higher energy;
- The Background cross-section is suppressed by 1/s.

The mono-photon process plays better at 240GeV or 10TeV lepton colliders.

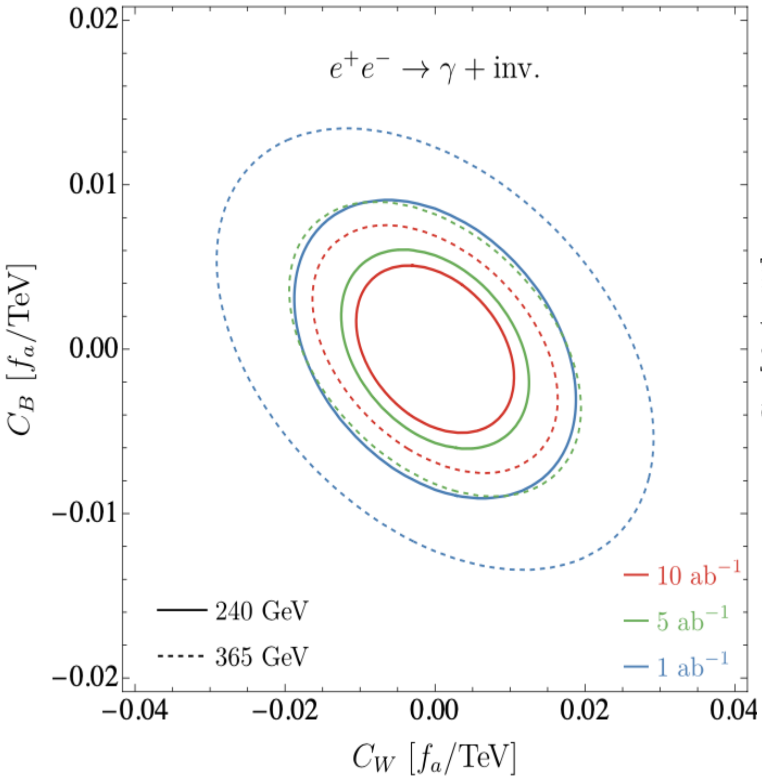

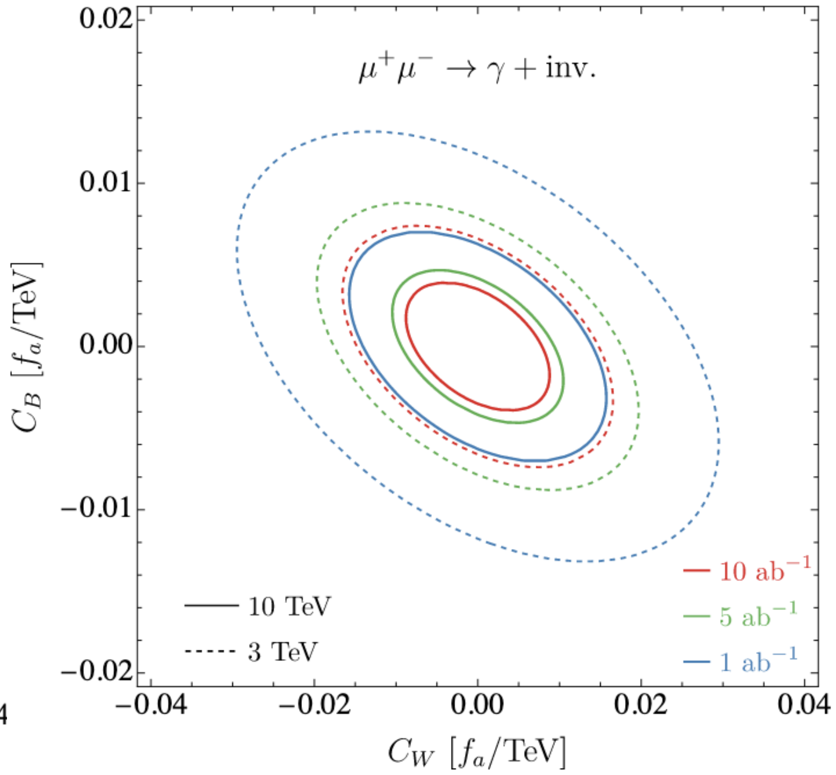

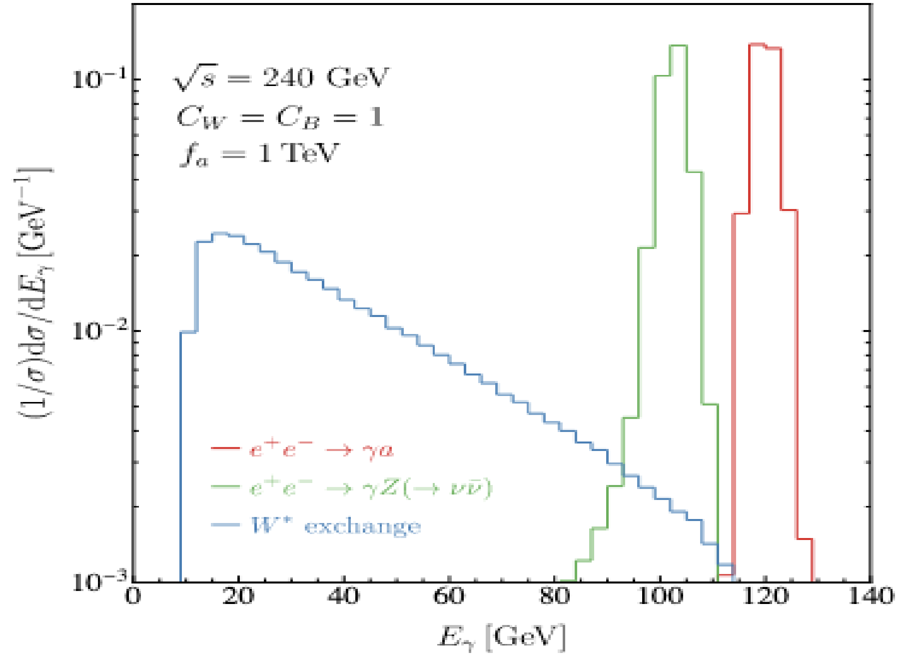

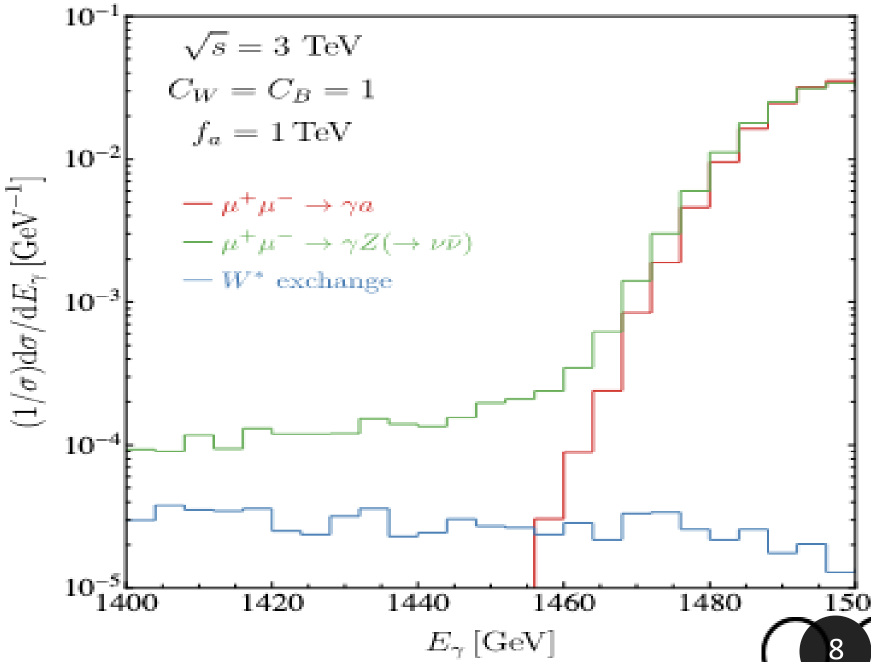

Tera-Z Phase Sensitivity

High Luminosity

At the Tera-Z phase of FCC-ee or CEPC, the mono-photon channel benefits from **high luminosity** (~100 ab^{-1}), **low background** and **resonant enhanced production x-section**.

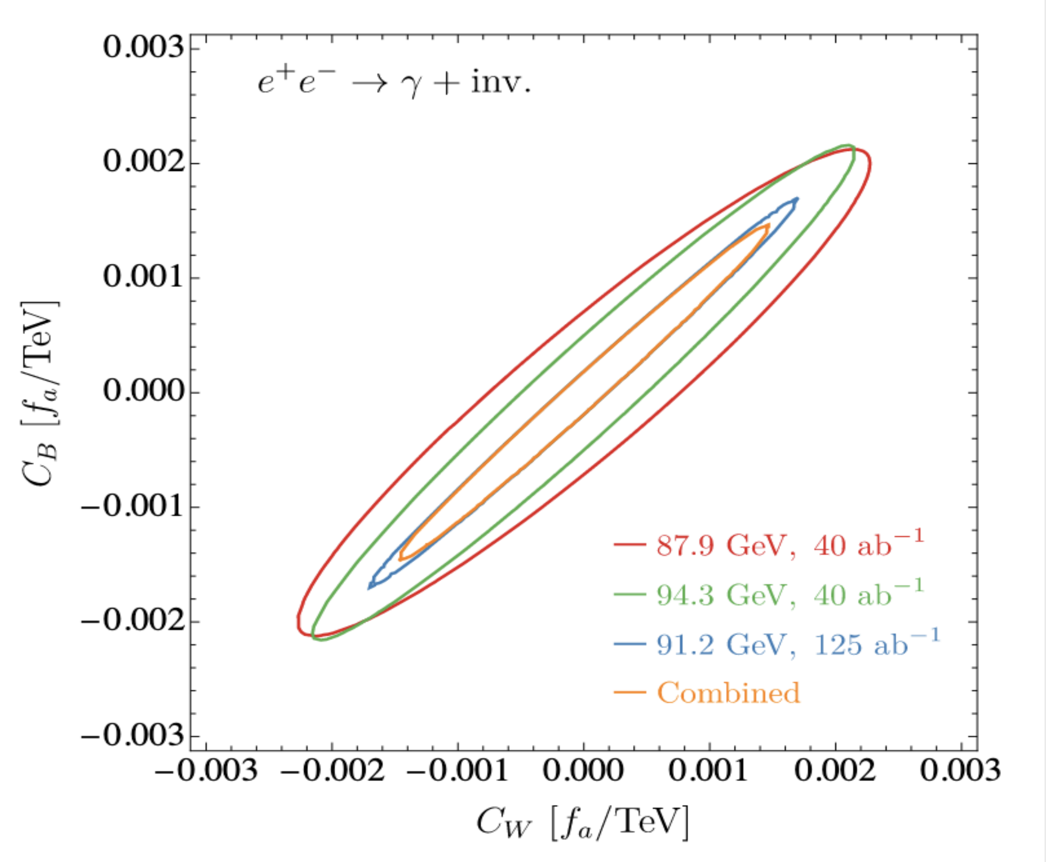

Mono-Z Production Process

Production Mechanism

ALP can also be produced with Z boson, leading to a mono-Z signature, which decays leptonically or hadronically.

Background considered

- di-Z: $\ell^+\ell^- \to Z(\to \ell\ell)Z(\to \nu\bar{\nu})$,
- di-W: $\ell^+\ell^- \to W^+(\to \bar{\ell}\nu)W^-(\to \ell\bar{\nu})$,
- W^* and γ/Z exchange: $\ell^+\ell^- \to \bar{\nu}_\ell \nu_\ell Z(\to \ell\ell)$ and $\ell^+\ell^- \to \ell^+\ell^- Z(\to \ell\ell)$.

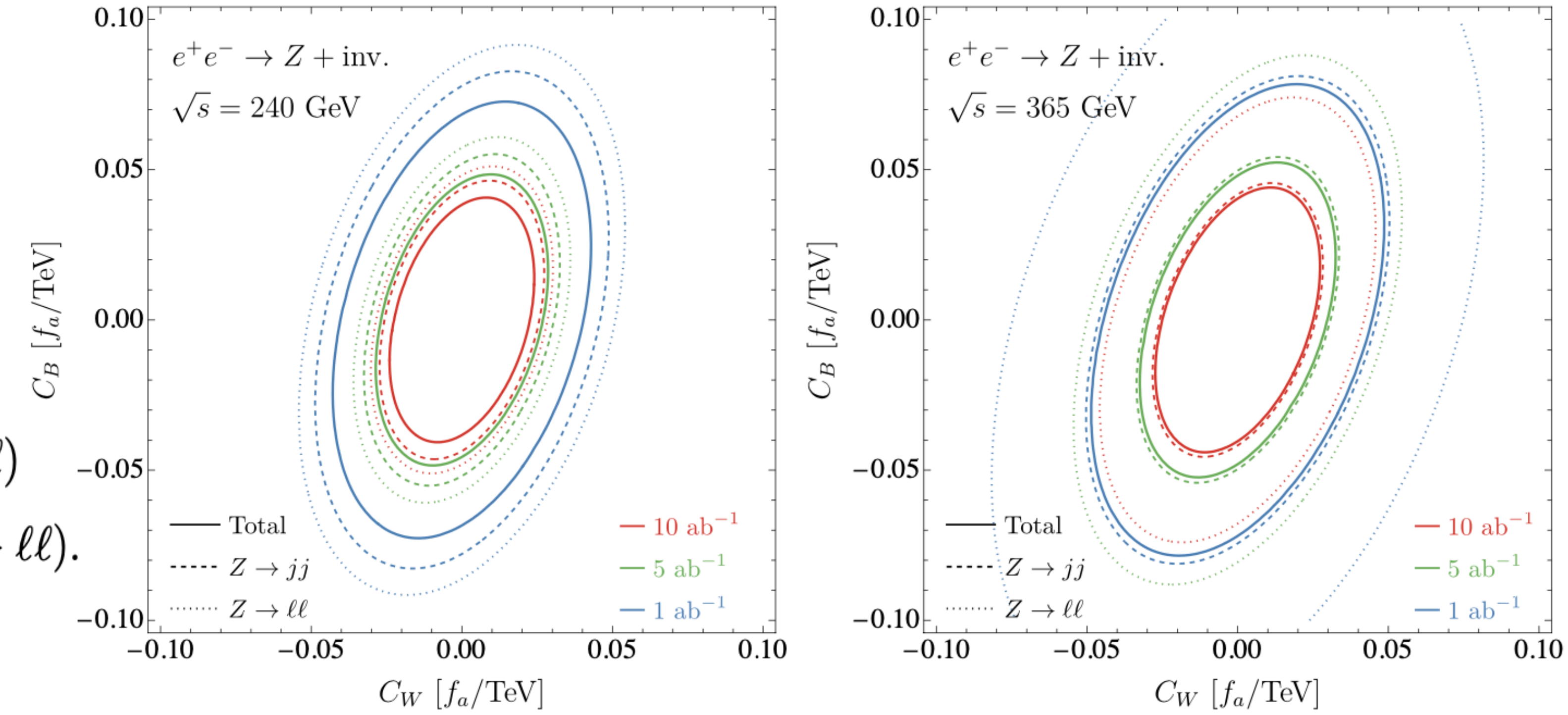

Experimental Significance

- The mono-Z channel is particularly useful for probing gaZZ and gaγZ, offering a robust method to constraint ALP couplings.
- The cross-section is significant at high energies and provides complementary sensitivity to mono-photon searches.

EW Vector Boson Scattering

Scattering Processes

- At higher energy colliders, EW VBS processes like $V_1V_2 \rightarrow V_3V_4$ are accessible.
- These processes can be used to probe g_{aZZ}, g_{aWW}, and $g_{a\gamma Z}$, as well as the $g_{a\gamma\gamma}$.
- ALPs contribute via off-shell exchange, then the x-sections are insensitive to the ALP mass.

W/Z VBS

- Since the W and Z are heavy, such channels can only be valid at higher energy colliders;
- Involve all ALP couplings with EW gauge bosons;

Light-by-Light Scattering

- Since the photon is massless, such scatterings are valid at CEPC/FCC-ee;
- The cross-sections are small and the sensitivity can not be competitive with Mono-photon.

EW Vector Boson Scattering

Sc

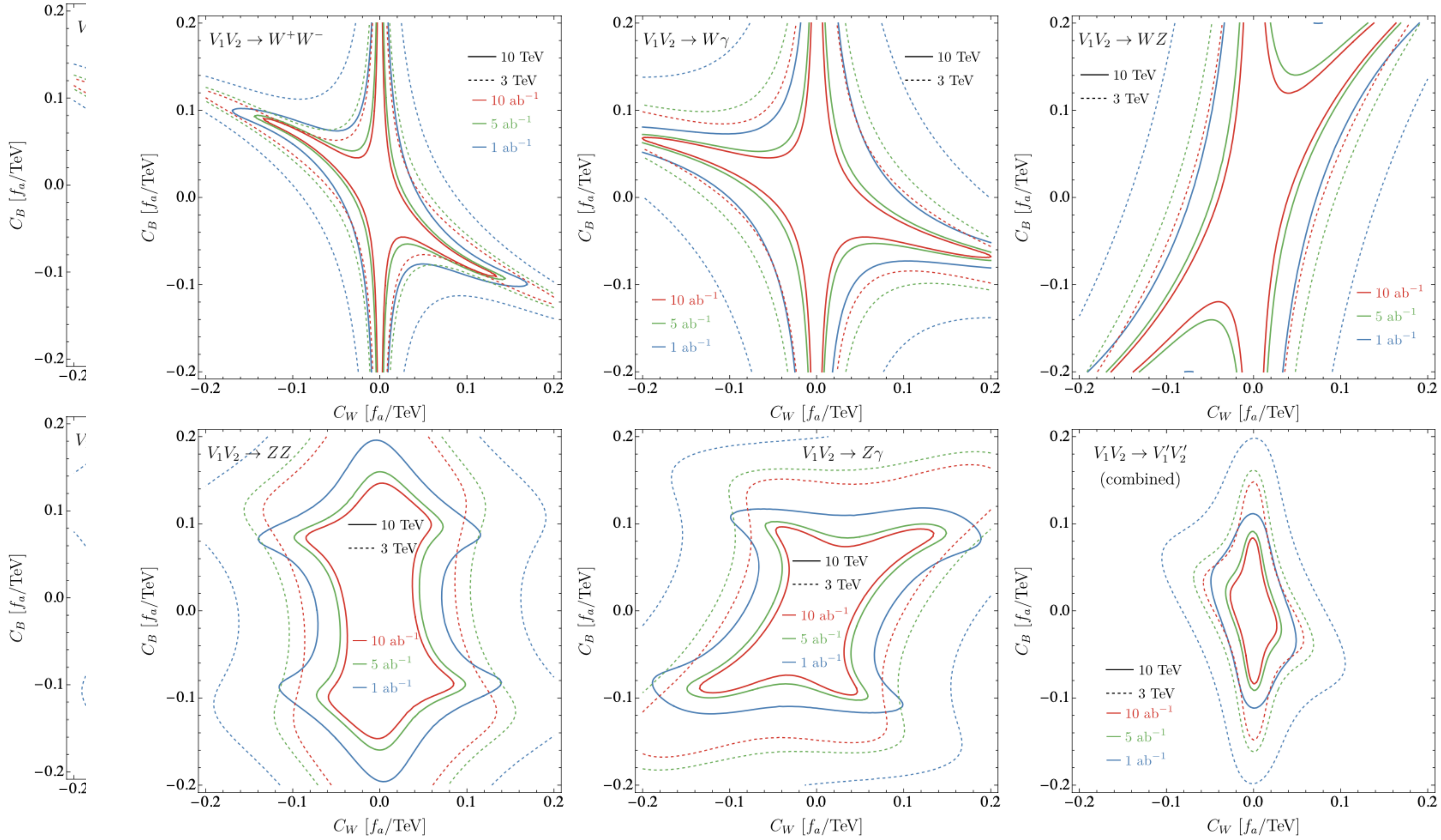

FCC-ee;

not be

Combined Sensitivity

Channel Contributions

- The mono-photon channel act better with lower energy collision;
- At higher energy colliders, the Mono-Z channel is complementary to Mono-photon;
- The VBS plays important role at ultra-higher energy collisions.
- The combination improves overall constraints at higher energy colliders.
- The gaZZ, gaWW, gaγZ, and gaγγ can be obtained.

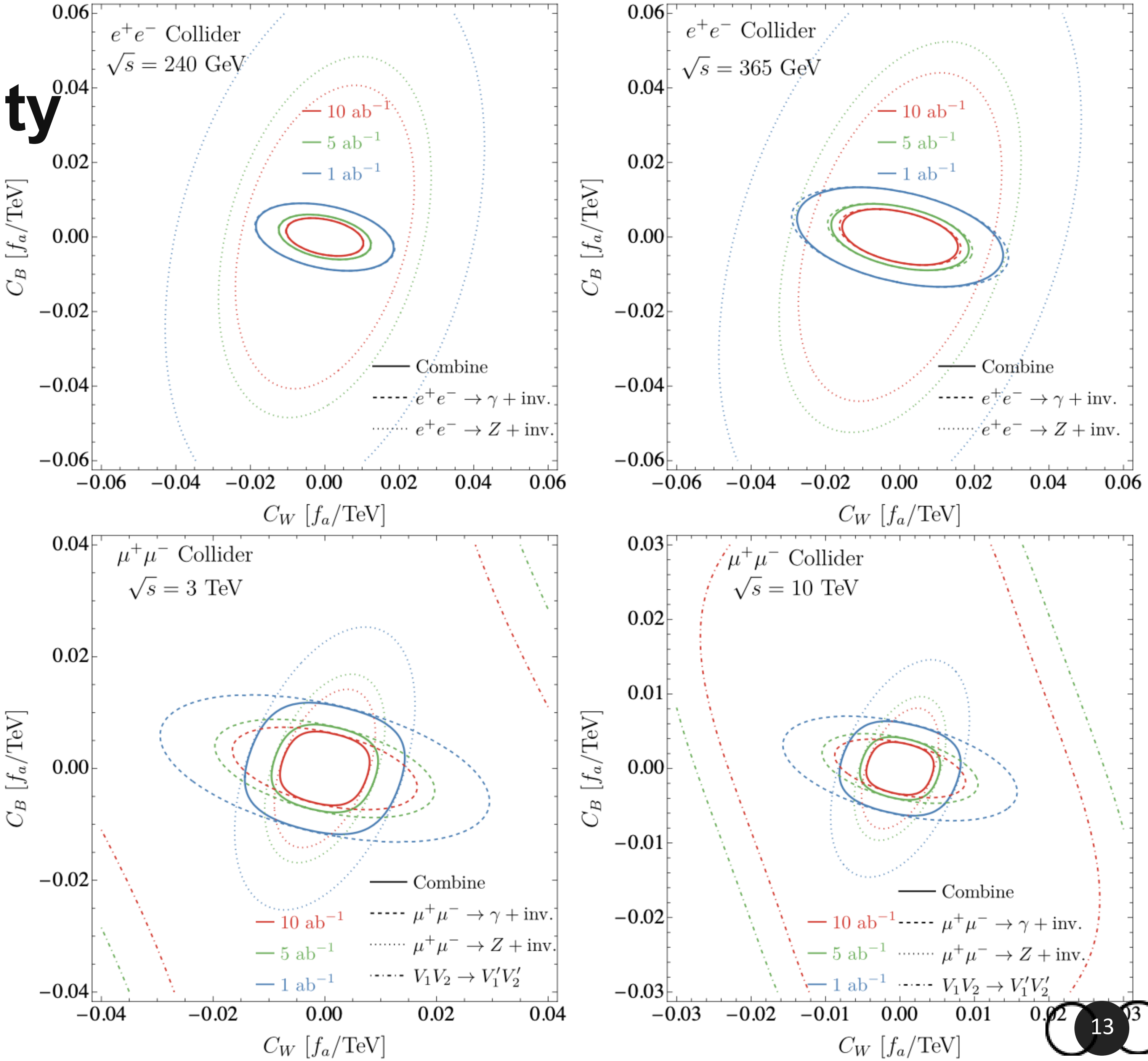

Combined Sensitivity

Channel Contributions

- The mono-photon channel act better with lower energy collision;
- At higher energy, the Mono-Z channel is complementary to Mono-photon;
- The VBS plays important role at ultra-higher energy collisions.
- The combination improves overall constraints at higher energy colliders.
- The gaZZ, gaWW, gaγZ, and gaγγ can be obtianed

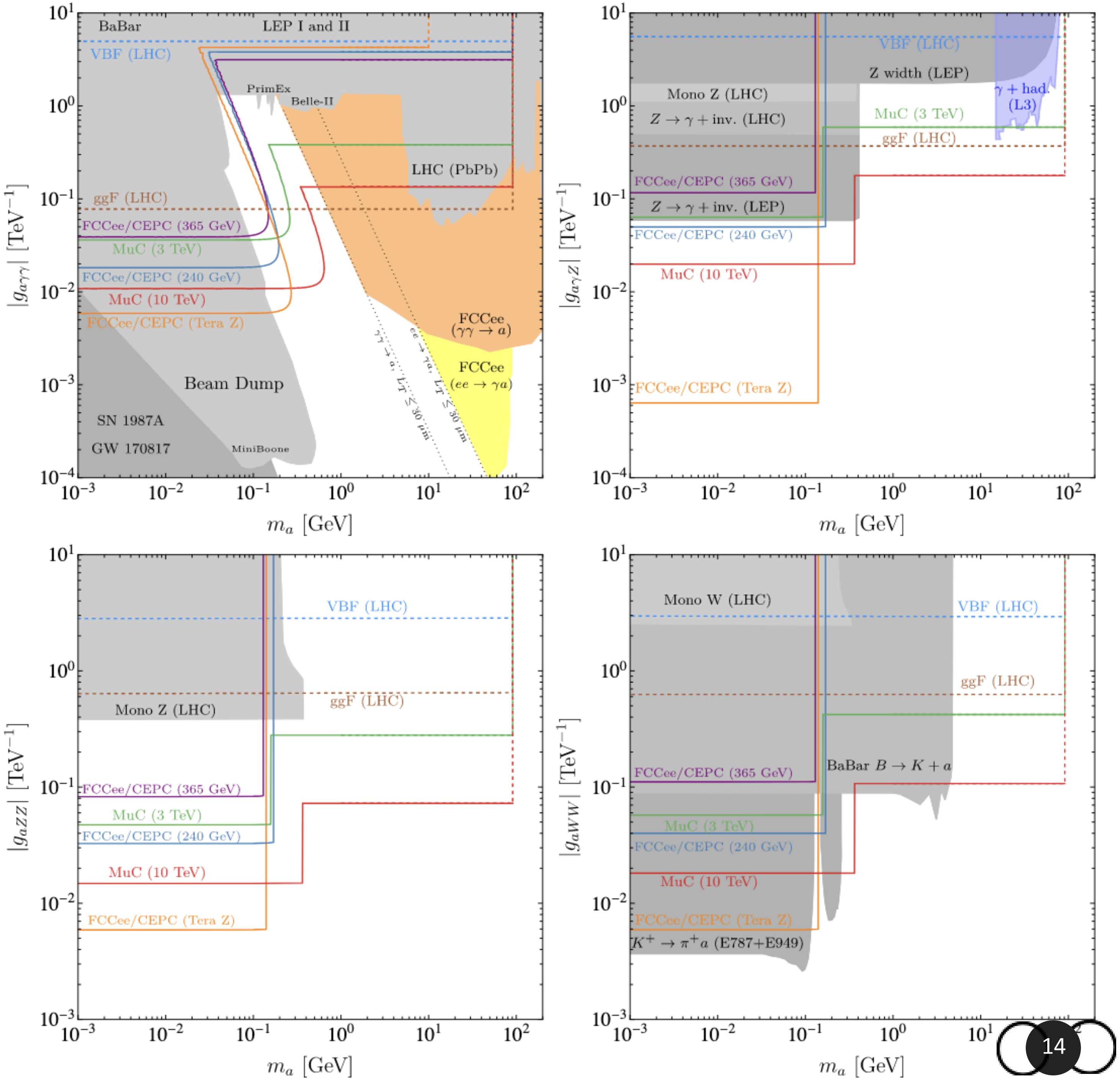

Conclusion

Future lepton colliders offer clean environments to probe ALP interactions with EW gauge bosons.

- The mono-photon process is the ideal channel to investigate the ALP couplings with EW gauge boson at CEPC/FCC-ee:
  - Due to the high luminosity, resonance enhanced cross-section and low background, the Tera-Z phase particularly sensitive to ALP interactions.
- The Mono-Z channel can be complementary to mono-photon channel:
  - It provides strong sensitivity to gaZZ and gaγZ;
  - The hadronic mode provides stronger bounds;
- VBS processes offer promising channels to probe the ALP couplings at high energies, with sensitivity extending to heavier ALP

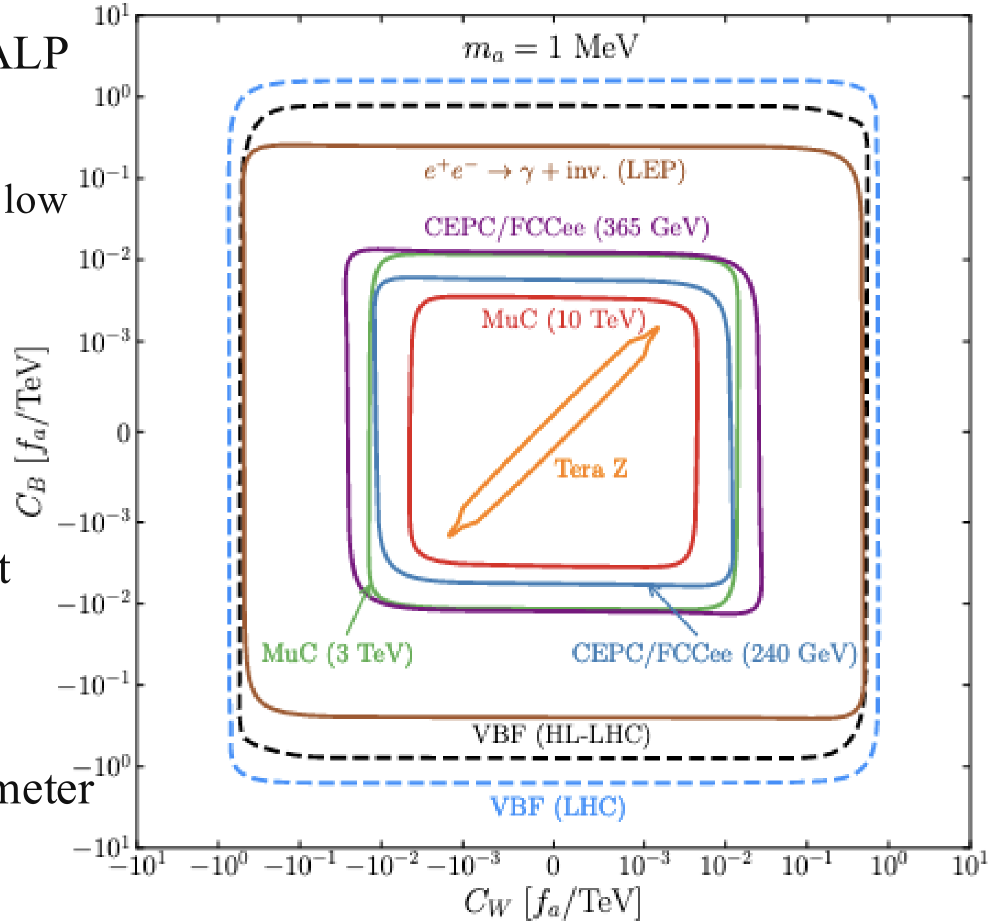

Combining all the channels ensures comprehensive coverage of ALP parameter space, and enhances the discovery potential of future lepton colliders.

THANKS FOR YOUR ATTENTION

Backup

Combined Sensitivity

The signal strength for the BSM effect is expressed as

$$\mathcal{S} = \sqrt{2(S+B)\log\left(1+\frac{S}{B}\right) - 2S},$$

where S is the number of signal events and B is the number of background events, and $\mathcal{S} = 1(2)$ corresponds the exclusion at 68% (95%) CL.

Combination Method

Constraints from mono-photon, mono-Z, and VBS channels are combined using a joint significance metric. Each channel contributes uniquely to the overall sensitivity.

$$\mathcal{S} = \sqrt{\mathcal{S}_{\gamma}^2 + \mathcal{S}_{Z}^2 + \mathcal{S}_{\text{VBS}}^2}$$

Mono-Photon/Z: Signal and Background

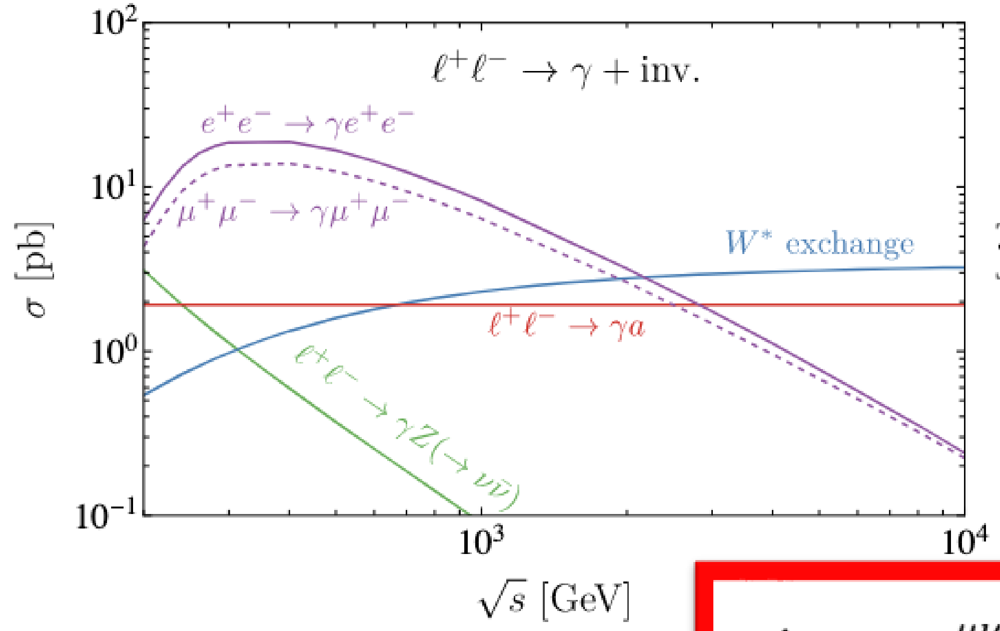

(a)

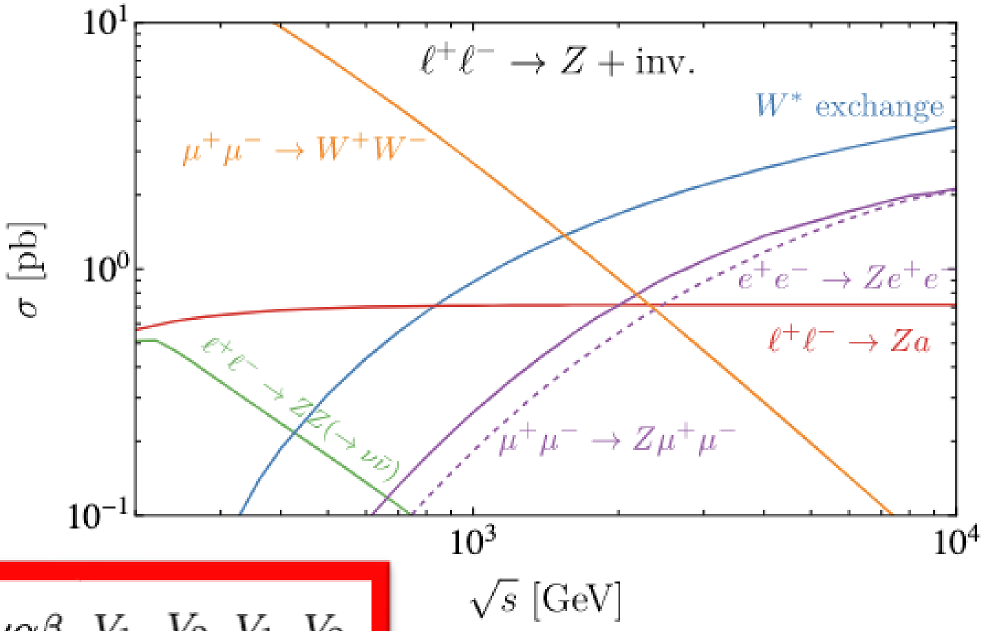

(b)

$$-ig_{aV_1V_2}\varepsilon^{\mu\nu\alpha\beta}p_\alpha^{V_1}p_\beta^{V_2}\epsilon_\mu^{V_1}\epsilon_\nu^{V_2},$$

Figure 3. The cross-sections of the signal and background processes for (a) mono-photon and (b) mono-Z production as functions of the collider energy. The signal cross-sections are computed with $C_W/f_a = C_B/f_a = 1\,\text{TeV}^{-1}$. The mono-photon production is evaluated with universal photon cuts $p_{T,\gamma} > 10\,\text{GeV}$ and $|\eta_\gamma| < 2.5$. The final-state leptons are required to be outside the detector coverage ($|\eta_\ell| > 2.5$) for the γ/Z exchange process $\ell^+\ell^- \to V + \ell^+\ell^-$. Additionally, an invariant mass cut of $M_{\ell\ell,\nu\nu} > 150\,\text{GeV}$ is applied to suppress on-shell $Z \to \ell^+\ell^-/\nu_\ell\bar{\nu}_\ell$ decays in the γ/Z and W exchange channels.

Mono-Photon/Z:

Event selctions

- Mono-Photon

e^+e^- 240 GeV	Basic	$p_{T,\gamma} > 60$ GeV	$E_\gamma > 115$ GeV
$\gamma + a$	1.93	1.58	1.56
$\gamma + Z(\nu\bar{\nu})$	1.83	0.704	2.12×10^{-4}
W^* exchange	1.04	0.0492	1.43×10^{-3}
$\mu^+\mu^-$ 3 TeV	Basic	$p_{T,\gamma} > 700$ GeV	$E_\gamma > 1450$ GeV
$\gamma + a$	1.92	1.64	1.64
$\gamma + Z(\nu\bar{\nu})$	9.11×10^{-3}	4.28×10^{-3}	4.28×10^{-3}
W^* exchange	2.97	7.71×10^{-3}	4.76×10^{-4}

- Mono-Z: hadronic (upper) and leptonic(lower) final states

Collider	e^+e^-		$\mu^+\mu^-$	
$\sqrt{s}$	240 GeV	365 GeV	3 TeV	10 TeV
$\|\eta_j\|^{\max}$	1.0	1.0	1.75	2.0
$p_{T,j_1}^{\min}$ [GeV]	60	75	550	1800
$p_{T,j_2}^{\min}$ [GeV]	40	40	–	–
$\Delta R_{jj}^{\max}$	2.0	1.8	–	–
$E_Z^{\min}$ [GeV]	123	180	1450	4800

Collider	e^+e^-		$\mu^+\mu^-$	
$\sqrt{s}$	240 GeV	365 GeV	3 TeV	10 TeV
$p_{T,\ell_1}^{\min}$ [GeV]	60	85	500	1600
$p_{T,\ell_2}^{\min}$ [GeV]	10	10	150	500
$E_{\ell\ell}^{\min}$ [GeV]	125	185	1450	4800
$p_{T,\ell\ell}^{\min}$ [GeV]	80	105	800	2200
$\Delta R_{\ell\ell}^{\max}$	2.3	2.0	0.4	0.15
$\|\eta_\ell\|^{\max}$	2.0	2.0	2.0	2.0

VBS

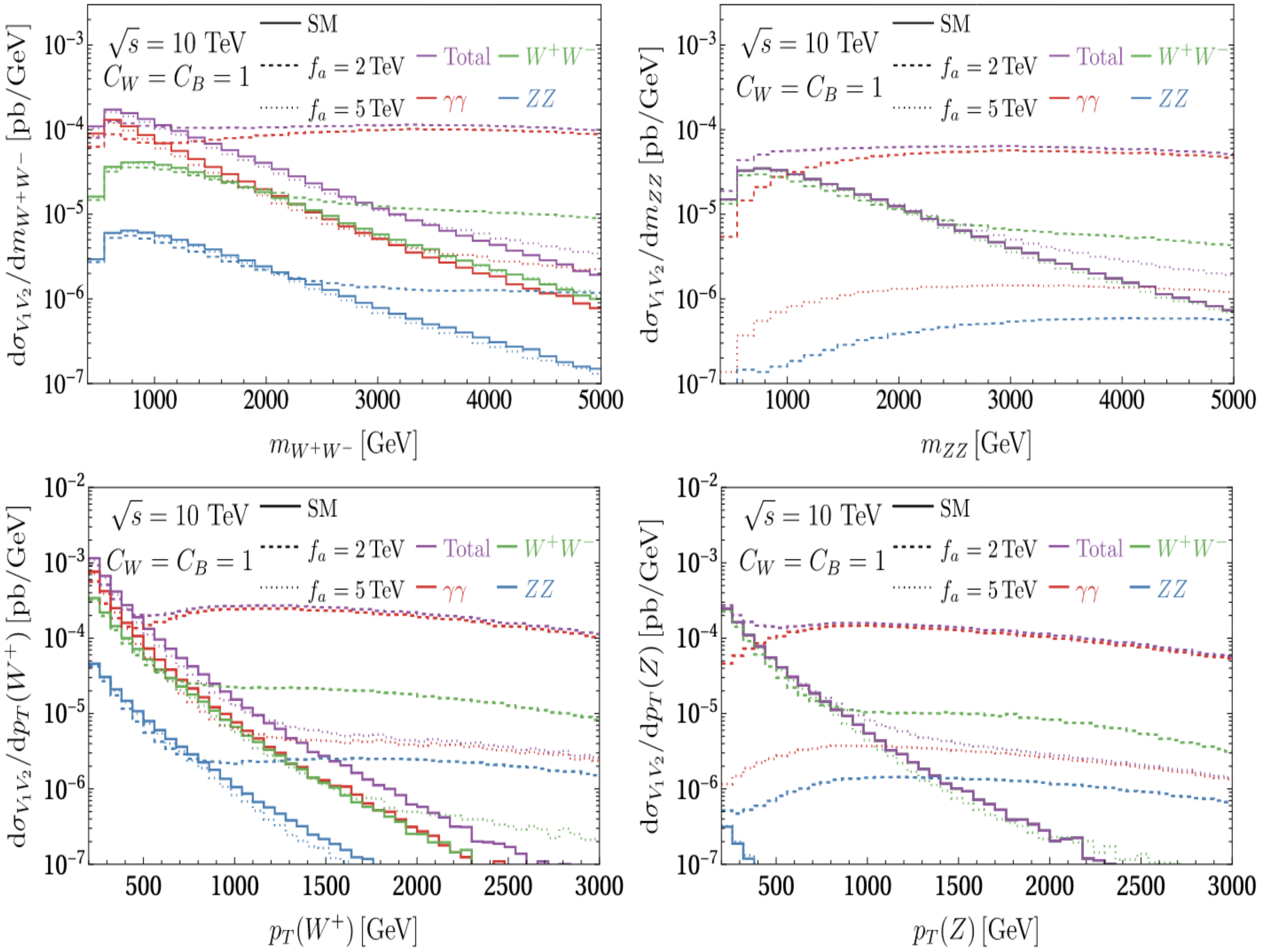

The ALP contribution exhibits a negative interference with the SM in the low pT (V) region. In contrast, at high pT (V), the BSM cross section exceeds the SM value. Based on this behavior, we divide the analysis into three kinematic regions:

- Near-threshold region: $p_T(V'_{1,2}) \in [150,\ 300]$ GeV
- Intermediate region: $p_T(V'_{1,2}) \in [300,\ 600]$ GeV
- High-p_T tail: $p_T(V'_{1,2}) > 600$ GeV

$$\mathcal{S}_{\text{VBS}} = \sqrt{\mathcal{S}^2_{\text{Near-threshold}} + \mathcal{S}^2_{\text{Intermediate}} + \mathcal{S}^2_{\text{High-}p_T}}.$$